Magnetoresistivity in the clustered state of $La_{0.7-x}Y_xCa_{0.3}MnO_3$ manganites

J. A. Souza and R. F. Jardim*
Instituto de Física, Universidade de São Paulo, Caixa Postal 66318, 05315-970, São Paulo, SP, Brazil
(Received 4 November 2004; published 7 February 2005)

We have performed a detailed characterization of both magnetic and transport properties of $La_{0.7-x}Y_xCa_{0.3}MnO_3$ ($x=0$, 0.05, 0.10, and 0.15) compounds. These measurements provide clear evidence for three temperature intervals in which the magnetic and transport properties are altered. The most notable is an intermediate regime called the clustered state, $T_C<T<T^*$, of phase coexistence involving the presence of both ferromagnetic (FM) and antiferromagnetic (AF) clusters and remnants of the high-temperature paramagnetic (PM) phase. The results further indicate a strong connection between spin cluster formation and the colossal magnetoresistivity effect. This magnetically clustered regime was observed to be altered by both magnetic field and disorder. The metal-insulator transition temperature T_{MI} and the width of the peak of $\rho(T)$ were found to change linearly with increasing disorder (Y content) and application of magnetic field with negative and positive derivatives, respectively. This indicates that disorder and application of magnetic fields (H) would cause the same effect but in an opposite way. We argue that correlated disorder effects influence both the shape and the magnitude of ρ versus T curves, as predicted theoretically. We have also inferred, from the computed excess of conductivity (or resistivity decrease) $\Delta\rho$ under decreasing T and application of H, that the electronic conduction process in the clustered state is described by a hopping mechanism. This result suggests two contributions to the electrical conductivity in the clustered state: (1) a semiconductinglike contribution and (2) hopping of carriers between FM metallic clusters.

DOI: 10.1103/PhysRevB.71.054404 PACS number(s): 75.47.Lx, 75.47.Gk, 72.20.Ee

I. INTRODUCTION

The $R_{1-x}A_xMnO_3$ perovskite manganites (where R is a rare-earth atom and A is divalent metal) exhibit interesting physical properties because of the strong interplay between lattice, charge, and spin degrees of freedom bringing about the colossal magnetoresistance effect (CMR).[1–3] Recent experimental[4,5] and theoretical[6,7] developments suggest a unified picture that confers a prominent role to the intrinsic inhomogeneities. These studies have indicated that the properties of these materials are related to intrinsic inhomogeneities due to disorder caused by the chemical-doping process widely used to control the hole density and the average hopping amplitude. Such an intrinsic disorder would induce spatially separated phases with different electronic and magnetic properties appearing far above the ferromagnetic (FM) transition temperature T_C.[7] Within this scenario, the large differences observed in the ground state of manganites are related to the existence of two different mechanisms leading to the phase separation. The level of disorder is the key variable defining the length scale of each phase and the metal-insulator transition is treated in a percolative framework where the conduction through metallic or insulating phases alternatively dominates the transport properties below and above the metal-insulating transition temperature, T_{MI}, respectively. Magnetoresistive properties in these systems are also explained as the result of altering the initial equilibrium between phases, the applied magnetic field favoring and enlarging the FM and metallic domains at the expense of the insulating ones.[7]

The understanding of both the electrical transport and the enhanced CMR effect in the paramagnetic state PM is still incomplete. Based on the transport data of these manganites, several attempts have been made in order to gain further information about the nature of the electronic conduction at high temperatures. The strong distortion of the MnO_6 octahedron contributes to the idea that the carrier transport at high temperatures is caused by the motion of the small-size lattice polarons.[8] De Teresa *et al.*[9] have shown, through small-angle scattering experiments, the occurrence of FM clusters within a PM matrix which grow in size but decrease in number with the application of magnetic fields. Thus, the CMR effect was believed to be due to the confinement of the charge carriers into finite FM clusters in the temperature interval $T_C<T<1.8T_C$.[9] Indeed, studies have indicated the existence of three regimes as a function of the temperature: (1) a high-T regime, where the system is PM and $\rho(T)$ has semiconductinglike behavior; (2) an intermediate regime $T_C<T<T^*$ with preformed clusters but with uncorrelated order parameters giving a globally PM state; (3) a FM regime, for $T<T_C$, in which clusters from (2) coalesce and percolate upon cooling to form a FM phase with metallic behavior.[10,11]

A better understanding of the mechanism governing both the magnetization and electrical resistivity and their evolution with doping should give better insight into the phase separation picture and be essential to the understanding of the microscopic origin of the CMR effect. Based on these arguments, we have studied a series of samples with composition $La_{0.7-x}Y_xCa_{0.3}MnO_3$ ($0\leqslant x\leqslant 0.15$) by using electrical resistivity, magnetization, and magnetoresistivity MR measurements. The results obtained in this work clearly indicate the presence of an intermediate regime in which magnetic clusters [FM and antiferromagnetic AF] develop and coexist with PM regions. The results further reveal a strong connec-

 ©2005 The American Physical Society

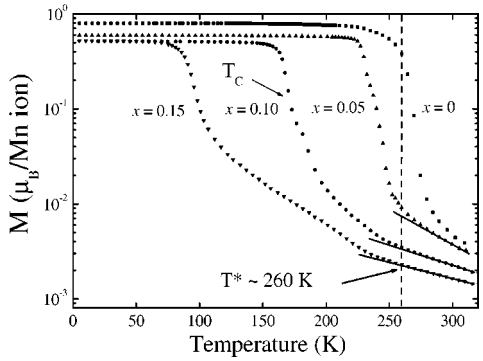

FIG. 1. Temperature dependence of the dc magnetization taken under 0.5 kOe. T_C=260, 230, 165, and 90 K for x=0, 0.05, 0.10, and 0.15, respectively. T_C is defined as the maximum inflection of M vs T. Lines are drawn as guides to the eye.

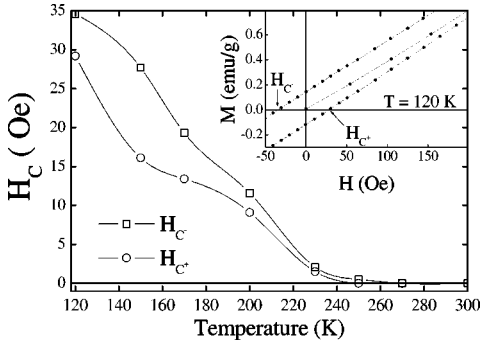

FIG. 2. Temperature dependence of the coercive field obtained from $M(H)$ measurements for the sample with x=0.15. The inset shows an expanded view of hysteresis loops taken at 120 K. Lines are guides to the eyes.

tion between spin cluster formation and dramatic magnetic field effects. Particularly, the preformation of the clusters, defining the clustered state, and its observation via macroscopic measurements, was found to play an important role in the semiconductinglike regime of these materials.

II. EXPERIMENTAL DETAILS

Polycrystalline samples of $La_{0.7-x}Y_xCa_{0.3}MnO_3$ (x=0.0, 0.05, 0.10, and 0.15) were prepared through a sol-gel method.[12] Powders prepared through this chemical route have better chemical homogeneity and smaller particle size than when using the standard solid-state reaction method. The powders were heat treated at 1000 °C and 1100 °C in air for 30 h, subsequently pressed into pellets, and subjected to a final heat treatment at 1200 °C in air for 30 h. The crystal structure was refined by the Rietveld method using the Fullprof program.[13] All the patterns were found to be similar indicating single-phase materials space group *Pnma*.[14] The oxygen contents of the samples were found to be constant through the series, in agreement with previous results.[15] Magnetization $M(T,H)$ measurements were performed in a commercial superconducting quantum interference device SQUID magnetometer. Four-probe electrical resistivity $\rho(T,H)$ measurements in applied magnetic fields up to 5 T were performed with a Linear Research LF-400 ac resistance bridge operating at 16 Hz.

III. RESULTS AND DISCUSSION

A. Magnetic properties

It is known that in mixed-phase manganites, metallic portions of the samples originate from the FM arrangement of spins that improves the electron conduction. Therefore, it is expected that the fraction of FM-metallic clusters increases as T decreases. The temperature dependence of the dc magnetization on a logarithmic scale for these samples is displayed in Fig. 1. The FM transition broadens with increasing Y content and T_C is shifted to lower T suggesting a weakening of the double exchange interaction between the Mn magnetic moments. The occurrence of broad magnetic transitions is believed to be associated with a large distribution of T_C.

A careful inspection of the $M(T)$ data in the low-temperature regime also indicates that increasing Y results in a gradual reduction of the saturation magnetization. This suggests either an incomplete ferromagnetic Mn moment alignment or the existence of an extra magnetic phase with a smaller saturation moment. On the other hand, it is plausible that such a decrease may be related to the development of nonferromagnetic clusters which may be paramagnetic or even antiferromagnetic (AF) in nature due to the disorder introduced by the partial substitution of La by Y. There are several experimental observations indicating the presence of distinct magnetic phases below T_C in these compounds. We have observed a paramagnetic component down to 20 K in ^{57}Fe-substituted $La_{0.6}Y_{0.1}Ca_{0.3}MnO_3$ through Mossbauer spectroscopy.[16] In addition to these findings, and important for further discussion, is the development of appreciable magnetic moments in samples with $x>0$ at $T^*\sim 260$ K, as inferred from the data shown in Fig. 1. This temperature T^* is close to $T_C\sim 260$ K of the $La_{0.7}Ca_{0.3}MnO_3$ sample, suggesting the development of ferromagnetism, even with short-range order, at high temperatures in these specimens. Information on the development of short-range FM order can be obtained through the Curie-Weiss law when it deviates from the expected linear behavior. However, χ^{-1} as a function of temperature was found to be nonlinear over the entire studied PM temperature range (from T_C to 380 K). Indeed, deviations from the Curie-Weiss behavior occur at temperatures much higher than measured here (600 K for the pristine sample, for example).[17]

In order to further investigate the development of short-range FM order, we have performed hysteresis loops in the sample with x=0.15 under small magnetic fields (±500 Oe) in the so-called paramagnetic regime. At 300 K, the curves exhibit features of a PM state as inferred from the linear M versus H dependence and the coincidence between M versus H curves taken upon increasing and decreasing H. However, below 250 K the curves display a small remnant magnetization and an intrinsic coercivity. Figure 2 shows the temperature dependence of the coercive field H_C and the inset displays an expanded view of the hysteresis loops taken at 120

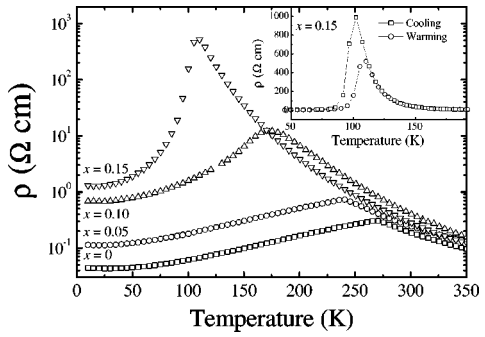

FIG. 3. Temperature dependence of the electrical resistivity for $La_{0.7-x}Y_xCa_{0.3}MnO_3$. $T_{MI}=265$, 240, 175, and 110 K for $x=0$, 0.05, 0.10, and 0.15, respectively. All curves were taken during increasing temperature. The inset shows ρ vs T for $x=0.15$ taken during increasing and decreasing T.

K. In the multilayers of spin valve and permalloy materials,[18] wherein the FM layers are coupled to AF layers, the hysteresis loops reflect the extent of the exchange coupling between the FM and AF layers. The coercivity of the FM layer increases due to the coupling with an adjacent AF layer. Since the phase-separated compositions of the manganites contain both FM and AF regions, they would be expected to show similar behavior.[19] Indeed, results obtained by Garcia-Hernandez *et al.*[20] in $La_{2/3}Ca_{1/3}MnO_3$ evidence FM and AF domains within a paramagnetic matrix correlated to the anisotropic lattice distortions above the FM transition. Moreover, it was proposed that the reported lattice distortions were attached to the presence of AF correlations, a result of a weakened double-exchange interaction operating along the locally distorted Mn-O-Mn paths. We suggest that these two ordered components FM and AF are the precursors of those clearly observed in the low-temperature region.[16,21] The width of hysteresis loops shown in Fig. 2 increases with decreasing temperature reflecting the effect of phase separation. The small differences in the coercive fields (H_C^+ and H_C^-) may be due to the pinning of a small fraction of AF interfacial spins to the FM domains. These results provide macroscopic experimental evidence of the phase separation above the FM transition, and are in agreement with neutron powder diffraction experiments.[20] Furthermore, they indicate the existence of an intermediate regime theoretically predicted by Burgy *et al.*[10] Another indication of the existence of correlated FM regions is the large temperature-dependent magnetoresistivity effect that is observed in the T region discussed here, as shown below.

B. Electrical resistivity and magnetoresistivity

We now focus our attention on the temperature dependence of the electrical resistivity $\rho(T)$ of this series, as shown in Fig. 3. All the $\rho(T)$ curves have similar behavior and exhibit a typical MI transition at different temperatures, in agreement with previous results.[22] The shape and width of the MI transition, ΔT_{MI}, are systematically altered with increasing Y content. As is clearly shown, T_{MI} coincides well with T_C in samples with low Y content. On the other hand, for the sample with $x=0.15$, $T_C\sim 90$ K is significantly lower than $T_{MI}\sim 110$ K, suggesting that the coupling strength between electrical and magnetic properties has been changed. Increasing Y content results in large magnitudes of $\rho(T)$ close to T_{MI} notably for the $x=0.15$ sample in which $\rho(T)$ is close to four orders of magnitude higher when compared with $\rho(T=350\ \mathrm{K})$. In the low-temperature regime $T<50$ K, the magnitude of $\rho(T)$ increases with increasing x. We suggest that this result is closely related to the observed decrease in the saturation magnetization with increasing Y discussed above and shown in Fig. 1.

The $\rho(T)$ data, taken under both increasing and decreasing temperatures for the sample with $x=0.15$ and displayed in the inset of Fig. 3, exhibit large thermal hysteresis, a feature hardly detected in the $\rho(T)$ curve belonging to the sample with $x=0$. The thermal hysteresis is a general signature of the first-order phase transition. The existence of a magnetic first-order transition usually gives an indication of the coupling of the spin system with the inhomogeneous electron-density distribution.[6] It suggests that the electronic structure of this sample is determined by the combination of the regions with locally higher charge density with FM spin correlations and by the remaining charge-depleted part, rather than simply by the average charge density. It is probable that charge arrangements in the charge-inhomogeneous state are expected to fluctuate in shape, especially at high temperatures where the clustering is dynamic. Moreo *et al.*[6] have considered different geometries for the FM region which can be classified as either stripes or clusters/droplets.

In addition to these findings, one can observe that the width of the MI transition, ΔT_{MI}, becomes narrower with increasing x, and consequently the electrical resistivity drop at T_{MI} is sharper for $x=0.15$ than for $x=0$ (see Fig. 4). Regarding the shape of the $\rho(T)$ curves, Moreo *et al.*[6] have proposed that disorder plays an important role in altering the character of the FM clusters and their dependence with temperature. To infer about effects caused by disorder, we have compared the width of both the MI transition ΔT_{MI} and the FM transition ΔT_C. As depicted in Fig. 1, the FM transition is sharper for the sample with $x=0$ and broadens significantly with increasing x. This observation suggests an increase of the random distribution of the FM coupling between Mn ions. However, ΔT_{MI} decreases with increasing x (see Fig. 5) which is the opposite of what occurs for ΔT_C. Thus, we have determined the width of the MI transition as a function of T_{MI}. ΔT_{MI} has been defined as being the full width at half maximum of the MI transition belonging to the $\rho(T)$ curve taken in zero applied magnetic field.[23] From the results of Fig. 5, one can observe that ΔT_{MI} decreases linearly with decreasing T_{MI}, or more appropriately, with increasing disorder.

Because of the relative variation of phases and the percolative character of the MI transition in manganites, T_{MI} is expected to increase with increasing applied magnetic field, a feature clearly observed in our magnetoresistivity data. The inset of Fig. 5 shows the ΔT_{MI} as a function of T_{MI}, which was now varied by the application of H for the sample with $x=0.15$. These results indicate that the shape (width) of the resistive MI transition changes linearly with increasing disorder and H and with both negative and positive derivatives,

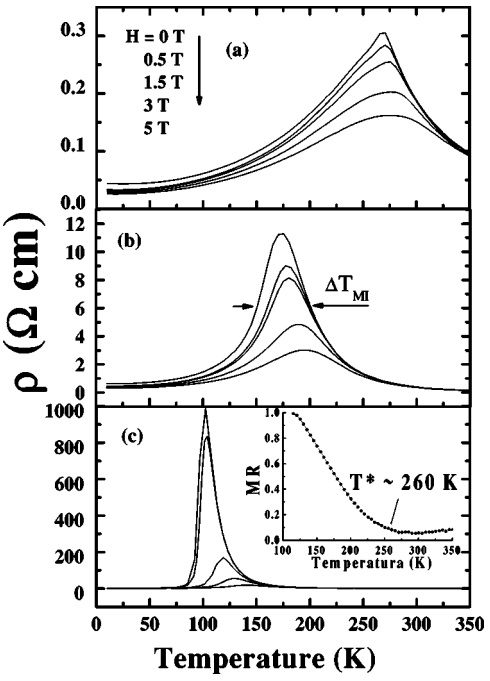

FIG. 4. Temperature dependence of the electrical resistivity under applied magnetic fields for $x=0$ (a), 0.10 (b), and 0.15 (c). The inset shows the MR$=[\rho(T,H=0)-\rho(T,H=3\ \mathrm{T})]/\rho(T,H=0)$ vs T for the sample with $x=0.15$.

respectively. Namely, whereas ΔT_{MI} and T_{MI} are decreased by increasing disorder, the magnetic field increases the magnitude of both. These observed results suggest that effects arising from both disorder and application of H in these samples are essentially the same, but they behave in an opposite manner. Thus, we infer that changes in both magnitude and shape of $\rho(T)$ curves close to T_{MI} reflect a complicated combination of size, shape, and resistivity changing of FM regions along with disorder effects as a result of Y substitution. In fact, both the shape and the magnitude of the peak at T_{MI} in ρ versus T curves have been related to the disorder strength in these manganites.[24] In addition, the ρ versus T curves shown in Figs. 4(a) and 4(c) are certainly well reproduced by Monte Carlo simulations when correlations in the quenched disorder are taken into account.[24] It has been suggested that the disorder can be propagated due to its cooperative nature through MnO_6 octahedra. Also, elastic interactions may be responsible for the appearance of superstructures in temperatures above T_C, as stripes, in the clustered state of these manganites.[24] From our results, it seems that the disorder strength, altered here by the partial substitution of La by Y, may vary the correlation of the quenched disordered state.

We have also observed that the $\rho(T)$ data for $T>T_{\mathrm{MI}}$ display a thermally activated form for all samples. Such behavior has been tentatively described by using three different models: the simple Arrhenius law,[25] the VRH model,[26] and the polaron model.[8] As an approach to determine the mechanism responsible for the transport properties of these manganites, we have excluded the Arrhenius activated model of our analysis. This was done because it may be considered a very crude approximation in these materials due to the strong interplay between lattice distortion/vibration and transport properties. In addition, since the conduction band is relatively narrow, with a bandwidth of about 0.1 eV, the localization phenomenon in manganites is important. On the other hand, optical measurements have indicated the opening of a real gap in the paramagnetic range of parent compounds,[27] so the VRH mechanism cannot be applied. Therefore, the polaron model has been applied for the whole insulating regime of each sample. The electrical resistivity as a result of hopping of adiabatic small polarons is given by

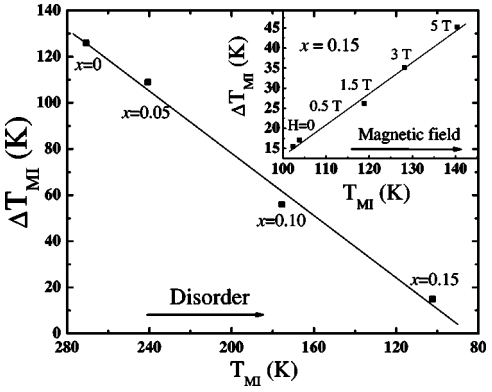

FIG. 5. ΔT_{MI} vs T_{MI} of each sample (increasing disorder). The inset shows ΔT_{MI} for the sample with $x=0.15$ as a function of T_{MI} which was now varied by increasing H.

$$\rho(T) = AT\exp\left(\frac{W_P}{k_B T}\right), \tag{1}$$

where W_P is the activation energy and k_B is Boltzmann's constant. We have found that this model fits the $\rho(T)$ data of the sample with $x=0$ very well, as shown in the inset of Fig. 6. On the other hand, samples with $x=0.10$ and 0.15 were found to exhibit two different regimes in the $\rho(T)$ curves above T_{MI}. For example, from Fig. 6 one observes that the $\rho(T)$ curve of the sample with $x=0.15$ deviates from linearity of the model at $T^*\sim 260$ K. Such a deviation indicates a crossover from activated carriers to another transport mechanism. This constitutes clear evidence of changes in the transport mechanism occurring near the temperature where the

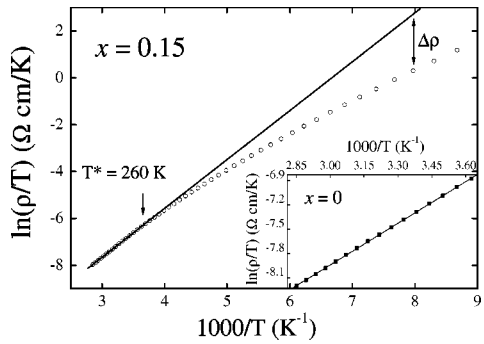

FIG. 6. Polaron model fitting for the sample with $x=0.15$. The inset indicates that the polaron model fits very well the electrical resistivity data of the sample with $x=0$. The lines are guides to the eye.

pristine sample ($x=0$) undergoes the MI transition. Another important result that corroborates the results described above is extracted from the MR measurements shown in the inset of Fig. 4(c). This figure displays the MR data, defined as $\mathrm{MR}=[\rho(T,H=0)-\rho(T,H=3\mathrm{T})]/\rho(T,H=0)$, for the sample with $x=0.15$ in the insulating regime, or more appropriately above T_{MI}. The results show that $\rho(T)$ is magnetic-field-independent in the temperature interval ranging from 350 K down to ~260 K, as indicated by small changes in the magnitude of MR. On the other hand, the MR effect is clearly observed below ~260 K. The relevant point here is that the MR effect is H-dependent below $T^*\sim 260$ K for samples with $x=0.10$ and 0.15. Moreover, it seems that both the change in the slope of $\rho(T)$ curves shown in Fig. 6 and the appearance of the MR effect are related to the occurrence of metallic clusters. The occurrence of these clusters, originated from short-range FM order, is in excellent agreement with $M(T,H)$ data shown above. These results indicate that the transport mechanisms at high temperatures in samples with high Y content can be separated at least into two temperature ranges: (1) from ~350 K down to $T^*\sim 260$ K, $T>T^*$; and (2) from T^* down to T_{MI}, $T_{\mathrm{MI}}<T<T^*$. Hereafter, we concentrate on the transport data of the sample with $x=0.15$, where these effects are more pronounced, as discussed below.

1. Electrical resistivity for $T>T^*$

The presence of small polarons implies the existence of local lattice distortions that localize charge carriers. In our samples, the partial substitution of La with Y certainly causes local lattice distortions due to the large difference of ionic radii. Moreover, not only the Y substitution effect but also the Jahn-Teller distortion about the Mn^{3+} ion is expected from its d^4 configuration in an octahedral environment. Considering only the T range from T^* to 350 K, the polaron model resulted in the best fit of the $\rho(T)$ data. It is important to point out that, in this temperature range, the $\rho(T)$ curves are essentially magnetic-field-independent [see Fig. 4(c)].

The W_P values obtained from the fitting were 140, 145, 170, and 190 meV for samples with $x=0$, 0.05, 0.10, and 0.15, respectively, and are in good agreement with previous reported values.[28] The prefactor A in Eq. (1) is expressed as $A=k_B/n_p e^2\omega_{\mathrm{op}}a_p^2$, where e denotes the electronic charge, a_p is the hopping distance of the polaron, n_p is the polaron concentration, and ω_{op} is the optical phonon frequency. If one assumes $\omega_{\mathrm{op}}\sim 10^{14}$ s^{-1},[8] and the polaron concentration to be equal to the concentration of carriers $n_p=1.2\times 10^{28}$ m^{-3}, then the polaron hopping distance can be estimated from the fitting parameter $A=7\times 10^{-7}$ Ω cm/K at room temperature to be $a_p\sim 6.5$ Å. This estimated value is comparable to the lattice parameters of these manganites and supports the conduction mechanism via polaron. Indeed, x-ray and neutron-scattering measurements directly demonstrate the existence of polarons in the PM regime of $La_{0.7}Ca_{0.3}MnO_3$.[29]

2. Electrical resistivity between T_{MI} and T^*

The discussion involving the $\rho(T)$ behavior between T_{MI} and T^* requires consideration about the magnetoresistivity data shown in Fig. 4. The $\rho(T)$ data are magnetic-field-independent in the high-temperature range $T>T^*$. On the other hand, $\rho(T)$ starts to change appreciably from the zero-field $\rho(T)$ curve by application of H at T^*, from which we define the intermediate temperature range, as shown in Fig. 7. This result indicates a strong connection between spin cluster formation and dramatic magnetic field effects. In other words, the development and presence of spin clusters strongly amplify the effect of magnetic field on the electronic properties of these systems. Indeed, this clustered state is argued to exhibit the colossal MR effect. Moreover, it was suggested that the combination of phase competition and the effect of correlations in quenched disorder creates the CMR effect in manganites.[24]

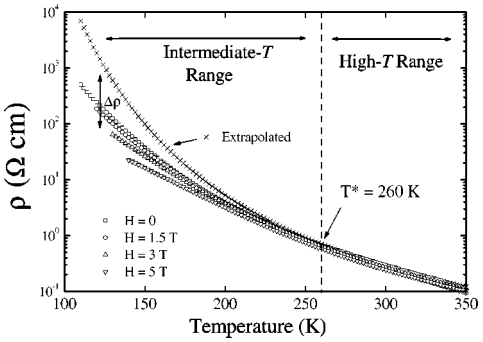

FIG. 7. ρ vs T for the sample with $x=0.15$ in the insulating regime at several applied magnetic fields. The $\rho_{\mathrm{ext}}(T)$ curve corresponds to the extrapolated low-T contribution of the polaron model fitted from 350 K down to 260 K. The excess of conductivity, defined as $\Delta\rho(T,H)=\rho_{\mathrm{ext}}(T)-\rho(T,H)$, is also indicated.

The MR results along with the deviation from the linearity in the polaron model at T^*, and the formation of magnetically ordered clusters at T^*, strongly suggest that a change in the transport process takes place at temperatures below $T^*\sim 260$ K. The $\rho(T)$ in this insulating region increases drastically (see Fig. 7) and there is no obvious easy channel for the flow of charge between clusters. The reduction of the electrical resistivity under applied magnetic field may reflect a rapid enhancement in the effective field experienced by localized charges when the magnetic clusters become mutually aligned by a magnetic field. In any event, the transport properties in such a clustered region are certainly complex. However, in order to gain further insight into the transport properties of these manganites, we have studied both qualitatively and quantitatively the behavior of the $\rho(T,H)$ curves between T_{MI} and T^*. Therefore, we analyzed the behavior of the conductivity excess (or the electrical resistivity decrease) ($\Delta\rho$) in the clustered state. First, we mention that two well established features of these manganites are relevant: the volume fraction of the FM metallic clusters or cluster size can be altered by either decreasing temperature or by applying magnetic fields. Within this context, we define $\Delta\rho$ as the difference between the extrapolated values of the electrical resistivity expected from the polaron behavior at low temperatures $\rho_{\mathrm{ext}}(T)$ and the measured $\rho(T,H)$ curves (see Figs. 6 and 7). Following the definition, $\Delta\rho(T,H=0)$ is due to the formation and increasing volume fraction of FM metallic

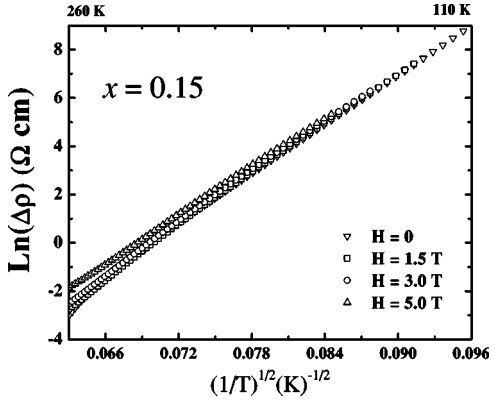

FIG. 8. Temperature dependence of the $\Delta\rho$ plotted by $\ln(\Delta\rho)$ vs $T^{-1/2}$ in the intermediate range of temperature for $H=0$, 1.5, 3.0, and 5.0 T.

clusters when the temperature is lowered, termed thermoresistivity. On the other hand, $\Delta\rho(T=\text{const},H)$ is related to the increasing volume fraction of FM metallic clusters induced by application of magnetic fields, termed magnetoresistivity. It is worth mentioning that when the temperature is varied and H is maintained constant, $\Delta\rho(T,H)$ includes these two contributions.

Considering the behavior of $\Delta\rho(T,H)$ as a function of T, we have found that it is essentially zero in the temperature range above $\sim$260 K and increases appreciably with decreasing T down to T_{MI}. From the temperature evolution of the $\Delta\rho$, one obtains a remarkable result: $\Delta\rho$ follows a thermally activated behavior. Further evidence of such a mechanism comes from the fact that $\Delta\rho$ is finite and appears simultaneously with the occurrence of magnetic clusters. To better clarify this point, we have attempted the following plots for the temperature dependence of $\Delta\rho$: $\ln(\Delta\rho)$ versus $T^{-\alpha}$ with $\alpha=1,1/4$, and $1/2$, which represent the semiconductor conductance in crystalline semiconductors, the variable range hopping conductance in amorphous semiconductors, and tunneling conductance in insulating granular systems, respectively.[30] From the results shown in Fig. 8, which displays the $\ln(\Delta\rho)$ versus $T^{-1/2}$ data, a linear trend is observed. The fitting procedure with $\alpha=1/2$ was first derived by Sheng *et al.*[31] when a tunneling process for the electrical conductance in insulating granular systems is considered. In that case, the main point related to this mechanism is that the conduction electrons can flow by tunneling between metallic granules. The morphology of either single crystals or polycrystalline manganite samples is actually granular. It can be considered as comprised of FM metallic clusters embedded in an AF/PM (insulating) matrix, as experimentally observed through Lorentz electron microscopy.[35] By taking into consideration the granular nature of manganites, a tunneling process between FM metallic regions is expected to occur at temperatures below T_C.[32,33] Based on the results described above, we suggest that a similar mechanism occurs in the clustered state. The tunneling process is also magnetic-field-dependent due to high spin polarization of these half-metallic materials. Thus, with increasing applied magnetic field, the magnitude of the tunneling process is enhanced due to its spin dependence nature.[34]

Based on the above discussion, we argue that changes in the behavior of $\rho(T)$ at $T^*\sim 260$ K are due to the development of FM metallic clusters within an insulating matrix. At this temperature, there is a smooth decrease in the electrical resistivity as a fraction of the material becomes metallic. This result is in qualitative agreement with neutron-scattering measurements[11] which suggest that T^* represents a phase transition from a polaronic liquid to a polaronic glass and at T_C the polaronic glass dissolves forming a long-range FM ordering and this behavior should track the electrical resistivity. Theoretical studies[10,36] have also revealed a temperature T^* much higher than T_C where uncorrelated clusters are formed and they claim that it is an expected feature in intermediate and low bandwidth manganites. Therefore, as the volume fraction of the metallic phase increases with both decreasing T and increasing H, these clusters begin to interact with one another via hopping of carriers. At sufficiently low temperatures, the volume fraction of the metallic phase attains the percolation threshold, and the sample undergoes a metal-insulator transition at T_{MI}. Such a picture is also in agreement with theoretical predictions in which intermediate-T clusters have much better electrical conductance than the insulating matrix.[10]

IV. CONCLUSION

The effects of disorder through the substitution of La by Y in polycrystalline samples of $La_{0.7-x}Y_xCa_{0.3}MnO_3$ ($x=0$, 0.05, 0.10, and 0.15) have been studied. The change in the conduction process, magnetic susceptibility, and the development of magnetoresistivity were found to be related to the formation and interaction between FM metallic clusters. The results clearly indicate an intermediate state $T_C<T<T^*$, termed a clustered state, that is more pronounced in samples with a higher content of Y, indicating that disorder plays an important role in the general physical properties of manganites. In this state, clusters with different magnetic properties (FM and AF) coexist within a PM insulating matrix amplifying strongly the effect of magnetic field on the transport properties. It can occur by generating huge effective fields seen by the carriers and through local coalescence of the clusters, which manifest themselves in the electrical resistivity of the system. The width of the metal-insulator transition changes linearly with increasing disorder and magnetic field with negative and positive derivatives, respectively. This indicates that disorder and H have the opposite influence on ρ. Furthermore, we have observed that the conductivity excess $\Delta\rho$, in the range $T_{\text{MI}}\lesssim T\lesssim 2.3\ T_{\text{MI}}$, under decreasing T and application of magnetic fields H, is described by a hopping mechanism in the clustered state. This result suggests that there are two contributions to the electrical resistivity: (1) one associated with semiconducting properties, and (2) one related to hopping of carriers between metallic clusters. Moreover, we have shown that the occurrence of these features can be inferred from an accurate analysis of macroscopic data such as magnetization and magnetoresistivity.

ACKNOWLEDGMENTS

The authors are indebted to J. J. Neumeier for useful discussions and valuable comments. This work was supported by the Brazilian agency FAPESP under Grant No. 02/01856-1 and 99/10798-0. R.F.J. was supported by the Conselho Nacional de Desenvolvimento Científico e Tecnológico CNPq under Grant No. 304647/90.

*Electronic address: rjardim@if.usp.br

[1] C. Zener, Phys. Rev. **82**, 403 (1951); J. B. Goodenough, Phys. Rev. **100**, 564 (1955); P. G. de Gennes, Phys. Rev. **118**, 141 (1960).

[2] R. von Helmolt, J. Wecker, B. Holzapfel, L. Schultz, and K. Samwer, Phys. Rev. Lett. **71**, 2331 (1993).

[3] A. J. Millis, P. B. Littlewood, and B. I. Shraiman, Phys. Rev. Lett. **74**, 5144 (1995).

[4] M. Uehara, S. Mori, C. H. Chen, and S.-W. Cheong, Nature (London) **399**, 560 (1999).

[5] M. Fäth, S. Freisem, A. A. Menovsky, Y. Tomioka, J. Aarts, and J. A. Mydosh, Science **285**, 1540 (1999).

[6] A. Moreo, S. Yunoki, and E. Dagotto, Science **283**, 2034 (1999).

[7] E. Dagoto, T. Hotta, and A. Moreo, Phys. Rep. **344**, 1 (2001).

[8] G. J. Snyder, R. Hiskes, S. DiCarolis, M. R. Beasley, and T. H. Geballe, Phys. Rev. B **53**, 14 434 (1996); M. Jaime, M. B. Salamon, M. Rubinstein, R. E. Treece, J. S. Horwitz, and D. B. Chrisey, *ibid.* **54**, 11 914 (1996); Guo-meng Zhao, K. Conder, H. Keller, and K. Muller, Nature (London) **381**, 676 (1996).

[9] J. M. De Teresa, M. R. Ibarra, P. A. Algarabel, C. Ritter, C. Marquina, J. Blasco, J. Garcia, A. del Moral, and Z. Arnold, Nature (London) **386**, 256 (1997).

[10] J. Burgy, M. Mayr, V. Martin-Mayor, A. Moreo, and E. Dagotto, Phys. Rev. Lett. **87**, 277202 (2001).

[11] D. N. Argyriou, J. W. Lynn, R. Osborn, B. Campbell, J. F. Mitchell, U. Ruett, H. N. Bordallo, A. Wildes, and C. D. Ling, Phys. Rev. Lett. **89**, 036401 (2002).

[12] R. F. Jardim, L. Ben-Dor, and M. B. Maple, J. Alloys Compd. **199**, 105 (1993).

[13] J. Rodriguez-Carvajal, Physica B **192**, 55 (1993).

[14] P. G. Radaelli, G. Iannone, M. Marezio, H. Y. Hwang, S.-W. Cheong, J. D. Jorgensen, and D. N. Argyriou, Phys. Rev. B **56**, 8265 (1997); L. M. Rodríguez-Martinez and J. P. Attfield, *ibid.* **63**, 024424 (2000).

[15] J. Fontcuberta, B. Martynez, A. Seffar, S. Pinol, A. Roig, E. Molins, J. Alonso, J. M. Gonzalez-Calbet, and X. Obradors, J. Appl. Phys. **79**, 5182 (1996).

[16] G. F. Goya, J. A. Souza, and R. F. Jardim, J. Appl. Phys. **91**, 10 (2002).

[17] S. B. Oseroff, M. Torikachvili, J. Singley, S. Ali, S.-W. Cheong, and S. Schultz, Phys. Rev. B **53**, 6521 (1996); C. Rettori, D. Rao, J. Singley, D. Kidwell, S. B. Oseroff, M. T. Causa, J. J. Neumeier, K. J. McClellan, S.-W. Cheong, and S. Schultz, *ibid.* **55**, 3083 (1997).

[18] D. V. Dimitrov, S. Zhang, J. Q. Xiao, G. C. Hadjipanayis, and C. Prados, Phys. Rev. B **58**, 12 090 (1998).

[19] Z. Li and S. Zhang, Phys. Rev. B **61**, R14 897 (2000).

[20] M. García-Hernández, A. Mellergard, F. J. Mompeán, D. Sánchez, A. de Andrés, R. L. McGreevy, and J. L. Martínez, Phys. Rev. B **68**, 094411 (2003).

[21] B. Hannoyer, G. Marest, J. M. Greneche, R. Bathe, S. I. Patil, and S. B. Ogale, Phys. Rev. B **61**, 9613 (2000).

[22] J. Fontcuberta, B. Martinez, A. Seffar, S. Pinol, J. L. Garcia-Munoz, and X. Obradors, Phys. Rev. Lett. **76**, 1122 (1996).

[23] In order to estimate ΔT_{MI}, we integrate ρ vs T curves and take the width at half maximum.

[24] J. Burgy, A. Moreo, and E. Dagotto, Phys. Rev. Lett. **92**, 097202 (2004).

[25] R. M. Kusters, J. Singleton, and D. A. Keen, Physica B **155**, 362 (1989).

[26] M. Viret, L. Ranno, and J. M. D. Coey, Phys. Rev. B **55**, 8067 (1997).

[27] A. Chainani, H. Kumigashira, T. Takahashi, Y. Tomioka, H. Kuwahara, and Y. Tokura, Phys. Rev. B **56**, R15 513 (1997).

[28] M. Ziese and C. Srinitiwarawong, Phys. Rev. B **58**, 11 519 (1998).

[29] C. P. Adams, J. W. Lynn, Y. M. Mukovskii, A. A. Arsenov, and D. A. Shulyatev, Phys. Rev. Lett. **85**, 3954 (2000).

[30] N. F. Mott and E. A. Davies, *Electron Processes in Non-Crystalline Materials* (Clarendon, Oxford, 1979).

[31] P. Sheng, B. Abeles, and Y. Arie, Phys. Rev. Lett. **31**, 44 (1973); B. Abeles, P. Sheng, M. D. Coutts, and Y. Arie, Adv. Phys. **24**, 407 (1975).

[32] H. Y. Hwang, S. W. Cheong, N. P. Ong, and B. Batlogg, Phys. Rev. Lett. **77**, 2041 (1996).

[33] H. Terashita and J. J. Neumeier, Phys. Rev. B **63**, 174436 (2001).

[34] S. L. Yuan, Z. C. Xia, L. Liu, W. Chen, L. F. Zhao, J. Tang, G. H. Zhang, L. J. Zhang, H. Cao, W. Feng, Y. Tian, L. Y. Niu, and S. Liu, Phys. Rev. B **68**, 184423 (2003); J. Blasco, J. Garcia, and J. Stankiewicz, *ibid.* **68**, 054421 (2003).

[35] T. Asaka, Y. Anan, T. Nagai, S. Tsutsumi, H. Kuwahara, K. Kimoto, Y. Tokura, and Y. Matsui, Phys. Rev. Lett. **89**, 207203 (2002); Y. Murakami, J. H. Yoo, D. Shindo, T. Atou, and M. Kikuchi, Nature (London) **423**, 965 (2003).

[36] A. Moreo, S. Yunoki, and E. Dagotto, Phys. Rev. Lett. **83**, 2773 (1999).